

DPAttack: Diffused Patch Attacks against Universal Object Detection

Shudeng Wu¹, Tao Dai^{1,2,*}, and Shu-Tao Xia^{1,2,*}

¹*Tsinghua Shenzhen International Graduate School, Tsinghua University, Shenzhen, China*

²*PCL Research Center of Networks and Communications,*

Peng Cheng Laboratory, Shenzhen, China

wsd19@mails.tsinghua.edu.cn, daitao.edu@gmail.com, xiast@sz.tsinghua.edu.cn

Abstract

Recently, deep neural networks (DNNs) have been widely and successfully used in Object Detection, e.g. Faster RCNN, YOLO, CenterNet. However, recent studies have shown that DNNs are vulnerable to adversarial attacks. Adversarial attacks against object detection can be divided into two categories, whole-pixel attacks and patch attacks. While these attacks add perturbations to a large number of pixels in images, we proposed a diffused patch attack (**DPAttack**) to successfully fool object detectors by diffused patches of asteroid-shaped or grid-shape, which only change a small number of pixels. Experiments show that our DPAttack can successfully fool most object detectors with diffused patches and we get the second place in the Alibaba Tianchi competition: Alibaba-Tsinghua Adversarial Challenge on Object Detection. Our code can be obtained from <https://github.com/Wu-Shudeng/DPAttack>.

1 Introduction

Object detection aims to locate objects (e.g. persons, dogs, flowers) from images. Recently deep neural networks (DNNs) [14, 3, 5, 11, 1, 10] have been widely and successfully used in object detection, which can be categorized into two-stage and one-stage methods. Faster RCNN [14] and Cascade RCNN [3] are two-stage methods that first use region proposal network (RPN) to obtain thousands of proposals and then classify these proposals into different classes. YOLO [1] and SSD [11] are one-stage methods which directly regress object bounding boxes and classify them.

One critical difference between two-stage and one-stage methods is that the sizes of their feature map are quite different. The feature map of Faster RCNN is down-sampled by $4\times$ from input images while that of YOLOv4 is down-sampled by $32\times$. As a consequence, the features of Faster RCNN have quite a smaller receptive field than those of YOLOv4. Meanwhile, two-stage methods like Faster RCNN contain an RoI pooling operation, which attends to all features within a proposal region. These features have a smaller receptive field and have equal contributions for proposal classification, so as to show more robustness to local perturbation. As our experiments have shown, two-stage detectors are harder to be attacked than one-stage detectors.

Adversarial attacks can fool models in lots of computer vision tasks, e.g. images classification [6, 4, 13], images segmentation [9, 7], face detection [17, 2] and object detection [16, 15, 8, 12]. Adversarial attacks against object detection can be divided into two categories: 1) whole-pixel attacks, which can add perturbations to all pixels in images under L_p constraints

*Corresponding author: Tao Dai and Shu-Tao Xia

Copyright © by the paper's authors. Use permitted under Creative Commons License Attribution 4.0 International (CC BY 4.0).

In: A. Editor, B. Coeditor (eds.): Proceedings of the CIKM2020 Analyticup Workshop, 23-10-2020, published at <https://www.cikm2020.org/>



Figure 1: Adversarial patches of asteroid-shaped (first row) and grid-shape (second row).

(e.g. L_1, L_∞); 2) patch attacks, which add perturbations to local pixels of a quite small area in images. However, Both whole-pixel attacks and patch attacks require a large area of images to add perturbations, which can be easily detected by human eyes or detectors. So we aim to change as fewer pixels as possible and make the number of patches (connected domains of changed pixels) less than 10.

To make our perturbation affect more features and at the same time change as fewer pixels as possible, we design a diffused patch of asteroid-shaped or grid-shaped (as shown in **Figure 1**). Specifically, we create asteroid-shaped or grid-shaped patches inside the bounding boxes of objects and using gradient-based methods (i.e. FGSM [6]) to update these patches iteratively. Meanwhile, both two-stage and one-stage detectors have nearly thousands of proposals. To avoid any proposal from being not attacked, we designed a special loss that pays more attention to unsuccessfully attacked proposals and can suppress introducing false positive proposals. We conclude the main contributions of this paper as follow:

- We design diffused patches of asteroid-shaped or grid-shaped, which can affect more features in the feature map of detectors at the cost of only changing a small number of pixels.
- Our attacking loss pays more attention to unsuccessfully attacked proposals and can suppress introducing false positive proposals.
- Experiments show that our method can successfully fool both two-stage and one-stage detectors at the cost of changing a small number of pixels. We get the second place in the Alibaba Tianchi competition: Alibaba-Tsinghua Adversarial Challenge on Object Detection.

2 Methodology

2.1 Problem Formulation

Two-stage object detectors use region proposal network (RPN) to obtain thousands of proposals and then classify them. One-stage detectors directly regress bounding boxes and scores of objects simultaneously and we define the pair of a bounding box and a score as a proposal as well. To this end, we define $P = \{p_1, p_2, \dots, p_N\}$ as proposals for both two-stage and one-stage detectors. Each element $P_i = \{x, y, h, w, s\}$ in P contains 5 components: left-top position, height, width of a bounding box, and scores of all predefined classes. Our attack only uses the scores of predefined classes and we use $S = \{s_i, \dots, s_N | s_i \in R^C\}$ to be the corresponding scores for proposals in P (C is the number of classes).

In order to affect more features in the feature map, we attach diffused patched to images. Besides, The patches must satisfy two conditions: 1) the number of patches is less than 10; 2) the total number of changed pixels is less than 2% of the total number of pixels in an image.

2.2 DPAttack: Diffused Patch Attack

In this section, we introduce our proposed diffused patch attack in detail. Choosing the positions of patches is the first problem of the diffused patch attack. Intuitively, attaching the patches inside the bounding boxes is most effective to fool detectors and our visualization of gradients verifies it. To this end, we use the centers of bounding boxes as centers of patch masks of asteroid-shaped or grid-shaped (as shown in **Figure 1**). The attacking loss aims to make scores of classes below a threshold and at the same time suppress introducing false positive proposals. We formulate the attacking loss as

$$L(x, M, \delta) = \sum_{i=1}^N \sum_{c=1}^C \max(0, f_i^c(x \cdot (1 - M) + \delta \cdot M) - t) \quad (1)$$

Here $x \in R^{3 \times h \times w}$, $M \in R^{3 \times h \times w}$, $\delta \in R^{3 \times h \times w}$ means input image, patch masks and values of patches respectively. $f_i^c(\cdot)$ is the function which generates the score for class c of the i -th proposal, and t is the threshold score to distinguish the categories of objects (excluding background). Only positive proposals can contribute to the loss, and false-positive proposals can be effectively suppressed. The details of the diffused patch attack can be referred to as **Algorithm 1**.

Input: model function $f(\cdot)$; an input image x ; bounding boxes $bboxes$; maximum iterations T ; score threshold t ; step α .

Output: the adversarial example x'

```

1: generate mask  $M$  by taking centers of  $bboxes$  as
   centers of the masks.
2:  $\delta \leftarrow \mathbf{0}, i \leftarrow 0, n \leftarrow 1$ 
3: while  $i < T$  and  $n > 0$  do
4:    $l \leftarrow L(x, M, \delta)$ 
5:    $\delta \leftarrow \delta - \alpha \cdot \text{sign}(\nabla_{\delta} L(x, M, \delta))$ 
6:    $\delta \leftarrow \max(0, \min(\delta, 255))$ 
7:    $n \leftarrow$  number of positive proposals
8:    $i \leftarrow i + 1$ 
9: end while
10:  $x' \leftarrow x \cdot (1 - M) + \delta \cdot M$ 
11: return  $x'$ 

```

3 Experiments

3.1 Dataset and Evaluation Metrics

The dataset is provided by the Alibaba Tianchi competition, Alibaba-Tsinghua Adversarial Challenge on Object Detection, and consists of 1000 images (500×500 in resolution) from test data of MSCOCO 2017.

We use multiple metrics to evaluate our proposed method. The first metric is overall score (**OS**) which have two aspects of consideration, number of suppressed bounding boxes and number of changed pixels.

$$S(x, x') = \left(2 - \frac{\sum_k R_k}{5000}\right) \cdot \left(1 - \frac{\min(BB(x), BB(x'))}{BB(x)}\right) \quad (2)$$

Here R_k is the number of perturbing pixels of k -th patch, $BB(\cdot)$ is the number of bounding box of objects in images. Perturbing less number of pixels (R_k) and suppressing more bounding boxes of adversarial examples $BB(x')$ can make overall score higher. Besides, we use success rate (**SR**) to evaluate the performance of our attack. We deem our attack successful if we suppress all bounding boxes in images. The ratio of bounding box (**BBR**) is the ratio between the number of bounding boxes with regard to original images and adversarial examples. **APP** is the average ratio between number of perturbing pixels and whole pixels of adversarial examples.

$$BBR = \frac{\sum_{i=1}^N BB(x'_i)}{\sum_{i=1}^N BB(x_i)} \quad (3)$$

$$APP = \frac{1}{N} \sum_{i=1}^N \frac{\sum_k R_k}{500 \times 500}$$

3.2 Overall Results

Table 1: Results of diffused patch attack of different shape against YoLov4 [1] and Faster RCNN [14]. The number s in Asteroid- s means scaling the size of bounding box of patches by s , e.g. 0.8. The numble l in grid- $l \times l$ means that there are l horizontal and vertical lines in the grid-shape patches. Ensemble means that we choose the adversarial examples of the highest overall score (OS) from all these kinds of patches.

	YOLOv4[1]				Faster RCNN [14]			
	SR	OS	BBR	APP	SR	OS	BBR	APP
asteroid-0.8	96.2 %	1515	2.76 %	0.89 %	65.4 %	1241	12.3 %	1.05 %
asteroid-1.0	100 %	1401	0 %	1.14 %	78.8 %	1203	7.6 %	1.27 %
grid-1x1	75 %	1423	18.62 %	0.45 %	15.3 %	906	39.5 %	0.55 %
grid-2x2	100 %	1457	0 %	0.87 %	61.5 %	1160	15.38 %	1.10 %
grid-3x3	100 %	1305	0 %	1.29 %	86.5 %	1076	8.6 %	1.47 %
grid-4x4	100 %	1158	0 %	1.54 %	84.6 %	1017	9.38 %	1.63 %
ensemble	98.3 %	1563	1.82 %	0.87 %	76.5%	1436	12.1 %	0.98 %

The attack performance of diffused patch attack can be inferred to **Table 1**. As our aforementioned analysis, the Faster RCNN [14] has features with a small receptive field and its RoI pooling operations take ensemble of features into consideration so as to be more robust than TOLOv4 [1]. The success rates (SR) for YOLOv4 can be nearly 100 % for most kinds of patches, while less than 85 % in most cases for Faster RCNN. Similarly, overall scores for YOLOv4 are higher than Faster RCNN, and bounding box ratios (BBR) are lower than Faster RCNN. Besides, the predefined bounding boxes are not the ground truth boxes but are from the results of YOLOv4 and Faster RCNN respectively, so APPs for them are different. In fact, Faster RCNN perturbing more pixels and obtain lower scores.

3.3 Visualisation of gradients

Intuitively, it is much more effective to attach the patches inside the bounding boxes of objects in images and we visualize the gradients of attacking loss with regard to the input image. The attacking loss are reformulated from equation (2) as follow:

$$p = x \cdot (1 - M) + \delta \cdot M$$

$$L(p) = \sum_{i=1}^N \sum_{c=1}^C \max(0, f_i^c(p) - t) \quad (4)$$

We visualize the gradients $\|\nabla_p L(p)\|_1$ by applying their transparent heatmap to the original image. As show in **Figure 2**, the gradients in the bounding boxes of objects are higher than those outside the bounding boxes. So it is more effective to put patches inside the bounding boxes.

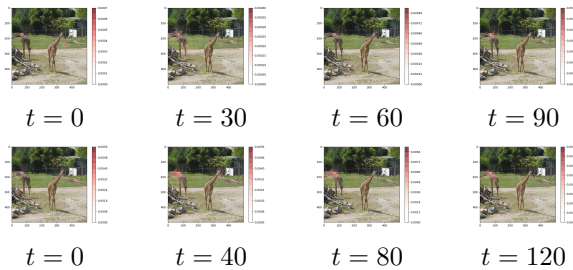


Figure 2: Visualisation of gradients for YOLOv4 (first row) and Faster RCNN (second row). t means iterations during the attack process.

4 Conclusion

In this paper, we proposed the diffused patch attack of asteroid-shaped or grid-shaped that can successfully fool both one-stage and two-stage detectors. Besides, our attack loss can pay more attention to positive proposals and suppress introducing false positive proposals. Experiments show that our proposed methods can successfully fool detectors at the cost of perturbing a small number of pixels and we get second place in the Alibaba Tianchi competition: Alibaba-Tsinghua Adversarial Challenge on Object Detection.

References

- [1] A. Bochkovskiy, C.-Y. Wang, and H.-Y. M. Liao. Yolov4: Optimal speed and accuracy of object detection. *arXiv preprint arXiv:2004.10934*, 2020.
- [2] A. J. Bose and P. Aarabi. Adversarial attacks on face detectors using neural net based constrained optimization. In *2018 IEEE 20th International Workshop on Multimedia Signal Processing (MMSP)*, pages 1–6. IEEE, 2018.
- [3] Z. Cai and N. Vasconcelos. Cascade r-cnn: Delving into high quality object detection. In *Proceedings of the IEEE conference on computer vision and pattern recognition*, pages 6154–6162, 2018.
- [4] N. Carlini and D. Wagner. Towards evaluating the robustness of neural networks. In *2017 IEEE Symposium on Security and Privacy (SP)*, pages 39–57. IEEE, 2017.
- [5] K. Duan, S. Bai, L. Xie, H. Qi, Q. Huang, and Q. Tian. Centernet: Keypoint triplets for object detection. In *Proceedings of the IEEE International Conference on Computer Vision*, pages 6569–6578, 2019.
- [6] I. J. Goodfellow, J. Shlens, and C. Szegedy. Explaining and harnessing adversarial examples. *arXiv preprint arXiv:1412.6572*, 2014.
- [7] J. Hendrik Metzen, M. Chaithanya Kumar, T. Brox, and V. Fischer. Universal adversarial perturbations against semantic image segmentation. In *Proceedings of the IEEE International Conference on Computer Vision*, pages 2755–2764, 2017.
- [8] M. Lee and Z. Kolter. On physical adversarial patches for object detection. *arXiv preprint arXiv:1906.11897*, 2019.
- [9] Y. Li, D. Tian, M.-C. Chang, X. Bian, and S. Lyu. Robust adversarial perturbation on deep proposal-based models. *arXiv preprint arXiv:1809.05962*, 2018.
- [10] T.-Y. Lin, P. Goyal, R. Girshick, K. He, and P. Dollár. Focal loss for dense object detection. In *Proceedings of the IEEE international conference on computer vision*, pages 2980–2988, 2017.
- [11] W. Liu, D. Anguelov, D. Erhan, C. Szegedy, S. Reed, C.-Y. Fu, and A. C. Berg. Ssd: Single shot multibox detector. In *European conference on computer vision*, pages 21–37. Springer, 2016.
- [12] X. Liu, H. Yang, Z. Liu, L. Song, H. Li, and Y. Chen. Dpatch: An adversarial patch attack on object detectors. *arXiv preprint arXiv:1806.02299*, 2018.
- [13] S.-M. Moosavi-Dezfooli, A. Fawzi, and P. Frossard. Deepfool: a simple and accurate method to fool deep neural networks. In *Proceedings of the IEEE conference on computer vision and pattern recognition*, pages 2574–2582, 2016.
- [14] S. Ren, K. He, R. Girshick, and J. Sun. Faster r-cnn: Towards real-time object detection with region proposal networks. In *Advances in neural information processing systems*, pages 91–99, 2015.
- [15] X. Wei, S. Liang, N. Chen, and X. Cao. Transferable adversarial attacks for image and video object detection. *arXiv preprint arXiv:1811.12641*, 2018.
- [16] C. Xie, J. Wang, Z. Zhang, Y. Zhou, L. Xie, and A. Yuille. Adversarial examples for semantic segmentation and object detection. In *Proceedings of the IEEE International Conference on Computer Vision*, pages 1369–1378, 2017.
- [17] X. Yang, F. Wei, H. Zhang, X. Ming, and J. Zhu. Design and interpretation of universal adversarial patches in face detection. *arXiv preprint arXiv:1912.05021*, 2019.